

Probing Particle Physics from Top Down with Cosmic Strings

Robert H. Brandenberger^{1,*}

¹*Physics Department, McGill University, 3600 University Street, Montreal, QC, H3A 2T8, Canada*

Making use of the wealth of new observational data coming from the sky it is possible to constrain particle physics theories beyond the Standard Model. One way to do this is illustrated in this article: a subset of theories admits cosmic string solutions, topologically stable matter field configurations. In these models, a network of cosmic strings inevitably forms in the early universe and persists to the present time. The gravitational effects of these strings leads to cosmological signatures which could be visible in current and future data. The magnitude of these signatures increases as the energy scale of the new physics involved in cosmic string formation increases. Thus, searching for cosmological signatures of strings is a way to probe particle physics model “from top down”, as opposed to “from bottom up” as is done using data from accelerators such as the Large Hadron Collider. Different ways of searching for cosmic strings are illustrated in this article. They include Cosmic Microwave Background temperature and polarization anisotropy maps, Large Scale Structure optical and infrared surveys, and 21cm intensity maps.

PACS numbers: 98.80.Cq

I. INTRODUCTION

Observational cosmology is in its golden age. Improved instrumentation has allowed observers to explore the universe to much greater depth than ever before. Optical and infrared telescopes yield maps of the distribution of galaxies to larger distances, microwave experiments have provided accurate cosmic microwave anisotropy (CMB) temperature maps, and promise to give us CMB polarization maps in the near future. There are also prototype 21cm telescopes which promise to yield three-dimensional intensity maps of the distribution of neutral hydrogen. This data is giving us precise information about the inhomogeneities in the universe.

As has been realized for some time, the seeds for the current structure of the universe had to have been laid down in the very early universe. Inflationary cosmology [1] is one paradigm for generating structure in the universe, and alternatives such as string gas cosmology [2], the Ekpyrotic scenario [3] or the “matter bounce” scenario [4] exist. These scenarios all involve physics at energy scales much larger than those currently explored in terrestrial accelerator experiments, scales which in fact could approach the Planck and superstring scales. Thus, it is natural to ask whether cosmological data can be used to explore particle physics beyond the Standard Model.

This article will survey one way of probing the connection between particle physics and cosmology. It is based on the fact that in a large class of particle physics theories beyond the Standard Model there are topologically stable field configurations called *cosmic strings* which are predicted to form in the early universe and which survive until the present time [5]. They correspond to lines in space with trapped energy density. The gravitational effects of this energy leads to distinct cosmological sig-

natures. Searching for these signatures is thus a way to probe particle physics beyond the Standard Model. The magnitude of the signals is proportional to the tension of the strings, which in turn is proportional to the square of the energy scale characteristic of the string. Hence, looking for cosmic strings in the sky is a way to probe particle physics “from top down”, i.e. with the tightest constraints on high energy physics processes. Searching for cosmic strings in the sky is thus an approach to test particle physics which is complementary to terrestrial accelerator experiments which test models “from bottom up”, i.e. where the tightest constraints are on low energy scales (see [6] for a more technical recent review of this topic).

In the following section, the basics of cosmic strings will be reviewed. Section 3 introduces the main effects by which strings lead to cosmological signatures. Sections 4 - 7 then focus on specific observational windows: large-scale structure, CMB temperature and polarization maps, and 21cm redshift surveys.

A word on notation: units in which the speed of light, Boltzmann’s constant and Planck’s constant are set to 1 will be used. The metric of the background homogeneous and isotropic space-time is

$$ds^2 = dt^2 - a(t)^2 d\mathbf{x}^2, \quad (1)$$

where t is cosmic time, \mathbf{x} are comoving spatial coordinates (coordinates painted onto the expanding space, coordinates which are constant for particles at rest in the expanding universe), and $a(t)$ is the scale factor which describes the expansion of space. A crucial length scale when considering the formation of structure in the universe is the *Hubble radius*, the inverse expansion rate. On sub-Hubble scales, fluctuations typically oscillate like they do in Minkowski space-time, on super-Hubble scales they are frozen in and squeezed (see e.g. [7] for a comprehensive review of the theory of cosmological perturbations and [8] for an introductory overview). As a final point, we remark that it is common in cosmology to la-

*Electronic address: rhb@physics.mcgill.ca

bel time t by cosmological redshift $z(t)$, a measure of the expansion of space between time t and the present time. The relation is

$$z(t) + 1 = \frac{a(t_0)}{a(t)}, \quad (2)$$

where t_0 is the present time.

II. COSMIC STRING BASICS

According to quantum field theory, our best description of matter at high energies, matter is described in terms of fields which live in space and evolve in time. A particle corresponds to a localized point-like fluctuation of the corresponding field, in the same way that a phonon is a localized point-like excitation in a crystal. Some crystals admit the possibility of stable defect lines, lines at which the orientation of the atoms in the crystal changes abruptly. In a similar way, certain quantum field theories allow the existence of stable field configurations with linear defects. Such defect lines are called *cosmic strings*. In the same way that not all crystalline materials admit defect lines, not all field theories admit cosmic strings. For example, the Standard Model of particle physics does not admit string configurations which are stable in the vacuum. However, many extensions of the Standard Model do admit such defects.

In the same way that in condensed matter systems which admit defect solutions, such solutions inevitably form during a fast crystallization process, in a quantum field theory model which admits cosmic string solutions, a network of such defect lines inevitably forms during the cooling process in the early universe. This is the famous Kibble mechanism [9].

In the simplest models which yield cosmic strings, the field configuration can be visualized as a vector of fixed length η which can point in any direction in a two-dimensional plane. For example, consider a complex scalar field ϕ with potential energy given by

$$V(\phi) = \lambda(|\phi|^2 - \eta^2)^2, \quad (3)$$

where η is the characteristic energy scale of the field theory and λ is a positive number (the so-called “self-coupling constant”). In the high temperature plasma of the very early universe, the scalar field will have sufficient thermal energy to cross the potential energy barrier at $\phi = 0$. However, when the temperature falls below a critical temperature T_c which is given by the energy scale η , the field no longer has enough energy. We say that at the temperature T_c a “phase transition” takes place. Below T_c , then in order to minimize the energy, the field would then like to be in a ground state with $|\phi| = \eta$. However, by causality the orientation of the ϕ vector in the complex plane must be random on scales beyond which no information has had time to propagate since the time of the Big Bang. Hence, on such scales there is a probability of order one that if one considers a circle \mathcal{C} in space

on that scale, then the field vector ϕ will circle the point $\phi = 0$. By continuity, it then follows that there needs to be at least one point on any disk bounded by \mathcal{C} with $\phi = 0$. These points connect to a line, and this is the center of the cosmic string. The energy density μ of the string is obtained by minimizing the sum of potential and gradient energies and is given by

$$\mu \simeq \eta^2, \quad (4)$$

where the dependence on the coupling constant λ cancels out. As the observant reader will have noticed, the above argument is based on causality and holds at all temperatures below the critical temperature, and thus at all times up to the present time. Thus, and this is the second aspect of the Kibble mechanism, in particle physics models which admit cosmic string solutions, a network of strings will persist until the present time.

The detailed form of the distribution of the cosmic string network must be studied by means of numerical simulations (see e.g. [10] for a selection of references on such simulations). However, the qualitative aspects can be derived using analytical considerations (see e.g. [11–13] for early reviews on the cosmology of cosmic strings). First of all, note that cosmic strings cannot have ends. Hence, they are either part of an infinite string network, or else there are loops. The infinite string network is described by a correlation length $\xi(t)$ which depends on cosmic time t and gives the mean separation and mean curvature radius of the long strings (in the “one scale” model of the string network, these two lengths are the same). Due to the tension, a curved string will typically have velocity in direction perpendicular to the string whose magnitude v is a significant fraction of the speed of light. As a consequence of the induced motion, there will be frequent string intersections which both produce string loops and lead to an increase in $\xi(t)$. On the other hand, by causality $\xi(t)$ is bounded from above by the horizon distance t (we are using units in which the speed of light is set equal to 1). The dynamics can be studied by means of a Boltzmann equation (see e.g. [13]) which in fact yields

$$\xi(t) \sim t, \quad (5)$$

where the proportionality constant must be determined numerically. It is found that a horizon volume has on the average N long strings passing through it, where $1 < N < 10$ based on simulations by different groups.

To summarize, it follows from analytical arguments that the cosmic string network will at times much later than the time of the phase transition take on a “scaling solution” according to which the statistical properties of the string network are time-independent if all lengths are scaled to the horizon distance t (see Figure 1 for an illustration of the scaling solution).

The cosmic string loops surviving at late times are the remnants of the interactions between long string segments. Their distribution also scales, and is characterized by a maximal radius αt , where α is a positive number of

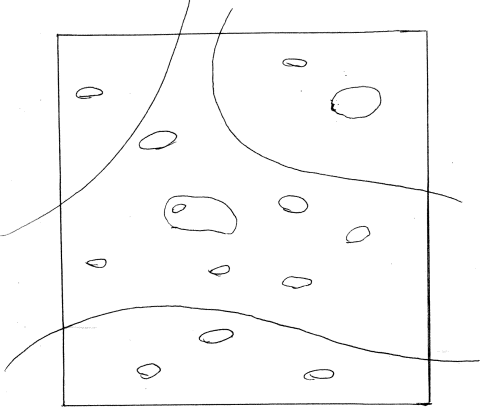


FIG. 1: Sketch of the cosmic string scaling solution. What is shown is the distribution of strings in a fixed Hubble volume (projected onto a plane).

the order but somewhat smaller than 1. As a function of radius R , the number density $n(R, t)$ of loops scales as $R^{-5/2}$ for loops formed before the time of equal matter and radiation (see e.g. [14]). String loops oscillate and emit gravitational radiation [15]. This effect leads to the fact that the number density $n(R, t)$ becomes constant below a cutoff radius given by

$$R_c = \gamma G \mu t, \quad (6)$$

where μ is the string tension, G is Newton's gravitational constant and γ is a real number whose value is determined in numerical simulations to be about 100.

Since a cosmic string arises in a relativistic quantum field theory, its mass per unit length is equal in magnitude to the tension. The gravitational effects of a string are hence proportional to μ . They are typically parametrized by the dimensionless constant $G\mu$ whose value is in the range $10^{-8} - 10^{-6}$ for cosmic strings formed in "Grand Unified" models of particle physics, and which are predicted to be in the range $10^{-12} - 10^{-6}$ for cosmic superstrings [16], fundamental strings which can be stabilized as macroscopic objects in certain string models [17].

Since in theories which admit cosmic strings a network of such strings survives until the present time, these strings will have observational consequences which can be searched for in observations (this was first realized in [5, 18, 19]). This will be the topic of the rest of this review.

III. MAIN EFFECTS

The network of cosmic strings at late times contains string loops and network of infinite strings with a correlation length $\xi(t)$ - we will call the latter the "long strings". Both loops and long strings lead to gravitational effects. Since, according to the current cosmic string evolution simulations most of the energy of the string network is in the string loops, the loops will dominate the cosmological effects. However, the long strings lead to more characteristic signatures and hence might be easier to detect in the sky. An important message of the following sections is that it is better to look for the signal of strings in position space rather than in Fourier space. The first reason is that in Fourier space the specific signals of the strings are washed out. The second reason is that (Fourier space) power spectra typically depend quadratically on the constant N which parametrizes our ignorance of the exact nature of the scaling solution, whereas the position space signals in the idealized case are independent on N .

A. Effects of string loops

A string loop will oscillate and slowly emit gravitational radiation. Viewed from a distance larger than the loop radius, the time-averaged gravitational effect of the loop is like that of a point mass of magnitude

$$M(R) = \beta \mu R, \quad (7)$$

where the deviation of the number β from 2π describes the difference of the loop shape from being circular. Hence, cosmic string loops will be the seeds of roughly spherical accretion (for simplicity we here neglect the initial center of mass motion of the loops). Before the time t_{eq} of equal matter and radiation, the accretion of baryons and dark matter is suppressed. Thus, the main growth starts at t_{eq} .

As long as there is enough matter to feed the growth, the growth about string loops will proceed independently. Loops of different radii R will lead to objects of different final masses $M_f(R)$

$$M_f(R) \simeq \beta \mu R \frac{z_{eq}}{z_{to}}, \quad (8)$$

where the last factor describes the gravitational accretion from time t_{eq} (with corresponding redshift z_{eq}) until the redshift z_{to} when accretion stops, e.g. the present time for small values of $G\mu$ and for loops sufficiently displaced from any larger loop.

The initial work on cosmic strings and structure formation [14] mostly focused on the effects of string loops, and made the hypothesis that cosmic strings were responsible for all of the inhomogeneities and anisotropies in the universe, and thus would be an alternative to cosmic inflation as an explanation for the origin of structure. As a consequence of the scaling distribution of cosmic strings, the spectrum of density fluctuations from strings is scale-invariant [20]. For a value of $G\mu \simeq 10^{-6}$ the spectrum would have the right overall amplitude to explain the large-scale structure (LSS) data.

However, the fluctuations start out as entropy fluctuations on super-Hubble scales, rather than adiabatic perturbations in the case of inflation. They are incoherent and active (i.e. the induced adiabatic component is growing on super-Hubble scales). As a consequence of these facts, the CMB anisotropies on small angular scales are predicted to be different from the results for primordial adiabatic fluctuations: there are no acoustic oscillations in the CMB angular power spectrum [21], but only one broad Doppler peak.

Once the acoustic oscillations in the CMB angular power spectrum were discovered by the Boomerang [22] experiment and later confirmed by data from the WMAP satellite mission [23] it became clear that cosmic strings could not account for all of the structure in the universe. This leads to an upper bound on the cosmic string tension. The most robust current bound on the string tension comes from the recent CMB angular power spectrum measurements, in particular the South Pole Telescope (SPT) [24], the Atacama Cosmology Telescope (ACT) [25] and the Planck mission [26]. The bound on the string tension from a combination of these experiments is [27] (see [28] for earlier limits)

$$G\mu < 1.5 \times 10^{-7}, \quad (9)$$

where the coefficient in fact depends on the constant N describing the string scaling solution (which has been mentioned earlier). This implies that cosmic strings can be responsible for at most about 5% of the power of density fluctuations in the current universe. The dominant source of inhomogeneities must be a different process such as inflation [29] or one of its alternatives (see e.g. [30] for a recent comparison between inflation and some of its alternatives).

From the particle physics point of view, however, there are good reasons to expect cosmic strings to be present, even if the universe underwent a period of inflation. In many supergravity models of inflation, strings are produced at the end of inflation [31], and in brane inflation models motivated by superstring theory, similarly a network of strings is the result of the termination of inflation [32]. In string gas cosmology, a network of cosmic superstrings may survive. Hence, looking for cosmological signals of strings provides a good way to probe particle physics beyond the Standard Model.

Cosmic string loops will accrete matter in a roughly spherical manner. String loops could, for example, con-

tribute to the formation of ultra-compact mini-halos embedded within a galaxy halo [33]. For a more general recent discussion of the role of cosmic string loops see e.g. [34]. However, in this article we will focus on signatures of long strings since their geometric patterns are more distinctive.

B. Kaiser-Stebbins effect

Because of the fact that a cosmic string has relativistic tension (tension equal in magnitude to the energy density), the gravitational effects of long straight strings are very special. There is in fact no local gravitational force exerted by the string. On the other hand, globally space is non-trivial - space perpendicular to a cosmic string is conical with a “deficit angle” α of magnitude proportional to the tension [35]

$$\alpha = 8\pi G\mu. \quad (10)$$

The conical structure of space perpendicular to a long string leads to lensing of light passing on different sides of the string. This, in turn, gives rise to a specific signature of long straight strings in CMB temperature maps [36, 37]: consider a source of light behind a string moving with velocity v_s in the plane perpendicular to the string, from the point of view of an observer at rest in the frame of the cosmological background. Light from this source will reach the observer on two different paths which pass on different sides of a string. There will be a relative Doppler shift in the frequency which the observer sees. Specifically, this effect applies to the CMB background radiation. Hence, a string will produce a line in the sky across which there is a relative temperature jump of magnitude

$$\frac{\delta T}{T} = 8\pi\gamma(v_s)v_s G\mu, \quad (11)$$

where γ_s is the relativistic gamma factor associated with the velocity v_s . For an illustration of this effect see Figure 2.

For cosmic strings formed during a phase transition in the early universe, the conical structure of space extends only a finite distance away from the string. As derived in [38], this distance is the time that light can travel between string formation and the time t which is being considered. Beyond that distance, space perpendicular to the string rapidly converges to being Euclidean. Hence, a string segment leads to a temperature surplus on one side of the string and a deficit on the other extending a distance corresponding to the comoving horizon at the time the light is passing by the string.

C. Cosmic string wakes

The conical structure of space perpendicular to a long straight string is also responsible for the second important effect, the “cosmic string wake”. We consider the

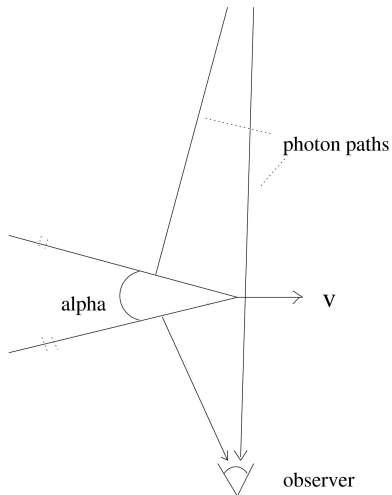


FIG. 2: Geometry of space perpendicular to a long straight string segment. Flattened out, there is a deficit angle whose magnitude is proportional to $G\mu$. A string moving with velocity v_s in transverse direction leads to a relative Doppler shift between photons passing on different sides of the string.

same string segment moving with velocity v_s in direction perpendicular to its tangent vector. It is moving through the cosmic gas. From the point of view of an observer behind the string, a velocity perturbation of the gas towards the “world plane” of the moving string (the plane spanned by the tangent vector to the string and the velocity vector v_s) is induced whose magnitude is

$$\delta v = 4\pi G\mu v_s. \quad (12)$$

Hence, a wedge-shape region of overdensity 2 behind the string is induced, the “wake” [39]. The wedge is a three-dimensional object. A string segment of length $c_1 t$, where c_1 is a constant, induces a wake of dimensions

$$c_1 t \times v_s \gamma_s t \times 4\pi G\mu \gamma_s v_s t, \quad (13)$$

where the second dimension is the depth and the third is the mean width, the width being zero at the point where the string is located, and twice the above value at the far end (see Fig. 3).

Once formed, a wake will grow in thickness by gravitational accretion, and it will expand in the planar di-

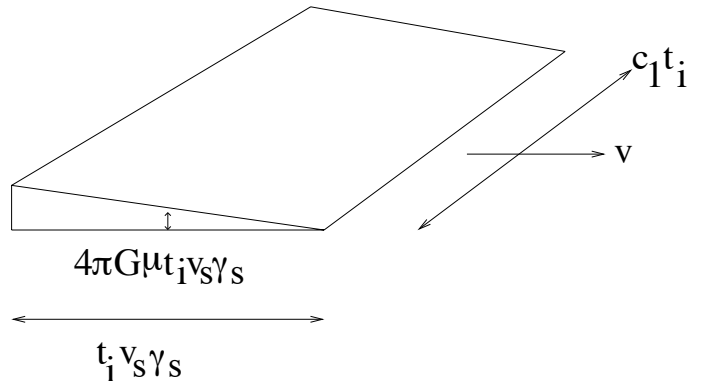


FIG. 3: The geometry of a cosmic string wake.

rections following the expansion of space. A long string present at time t_i (taken to be larger than t_{eq}) will create a wake whose physical dimensions at a later time t will be

$$c_1 t_i \frac{a(t)}{a(t_i)} \times v_s \gamma_s t \frac{a(t)}{a(t_i)} \times 4\pi G\mu \gamma_s v_s t_i \left[\frac{a(t)}{a(t_i)} \right]^2, \quad (14)$$

where the extra factor of $\frac{a(t)}{a(t_i)}$ in the third term comes from the growth of the width via gravitational accretion. The magnitude of this factor is easy to understand: it represents the linear cosmological perturbation theory growth of fluctuations. An improved derivation is based on the Zel’dovich approximation [40]. The thickness is defined as the physical radius of the mass shell which has just “turned around” and is beginning to collapse onto the central plane of the wake (initially every mass shell of particles above the wake is moving away from the wake because of cosmological expansion. The Zel’dovich approximation has been applied to cosmic string wakes in [41].

A key point is that cosmic string wakes correspond to nonlinear structures present already at the earliest times. This is in contrast to what happens in theories with Gaussian fluctuations such as those produced by inflation. In those theories fluctuations remain in the linear regime until times close to the epoch of reionization at redshifts of about 10. Hence, observational windows which probe nonlinear structures at high redshifts are more likely to find signatures of cosmic strings than surveys which probe cosmological structures at the present time.

IV. COSMIC STRINGS AND LARGE-SCALE STRUCTURE

In this section we will discuss signatures of cosmic strings in the large-scale structure observed through optical and infrared telescopes. We will focus on the role of the infinite string network since the long strings give rise to more distinctive geometrical patterns.

The long strings form a network of infinite extent. However, for analytical studies it is convenient to break up this network into a set of segments, each of length $\xi(t)$. As the infinite strings self-intersect and split off loops, the set of string segments changes. The time scale for string intersections is the Hubble expansion time scale t . Hence, string segments can be viewed as statistically independent on time scales larger than t . This idea gives rise to a toy model [42] for the distribution of long strings: we divide the time period under consideration (usually starting either at t_{eq} or else at the time t_{rec} of recombination and ending at the present time t_0) into Hubble time steps. In each time step (with initial time t_i , where i is the index of the time step), we take a fixed number N of straight string segments of length $\xi(t)$, and moving with velocity v_s . The centers, orientations, and velocity unit vectors are chosen at random.

Each string segment present at time t_i will produce a wake whose dimensions at a later time t are given by (14). The wakes will thus imprint a planar topology to the distribution of dark matter in the universe. In the “old days” of cosmic string cosmology the effects of wakes on the large-scale structure of visible matter was analyzed in many works, e.g. in [43]. Since there is only logarithmic growth of the density fluctuations before t_{eq} , the time interval to consider for studies of large-scale structure is the interval between t_{eq} and the present time. As a consequence of the scaling distribution of the string network, the overall power spectrum of induced density fluctuations is scale-invariant [14]. The specific signatures of cosmic strings cannot be seen in the two point correlation function, but only in non-Gaussian statistics. A better approach than naively computing three- and four-point correlation functions is to look at topological statistics such as Minkowski functionals [44]. This has been done in some early studies in [45].

For the small values of $G\mu$ which are now allowed by the bounds on the cosmic string tension, it was recently shown that halos which are induced by the accretion of matter onto wakes are too small and have too low a temperature to induce star formation. Hence, they will be difficult to detect directly [46], in spite of the fact that at higher redshifts the power spectrum of nonlinear matter becomes dominated by the string wakes. A more detailed study of this issue is in preparation [47].

V. CMB TEMPERATURE ANISOTROPIES FROM STRINGS

The cosmic microwave background (CMB) provides an image of the distribution of matter at the time t_{rec} of recombination, a time when the fluctuations are in the linear regime and precise analytical calculations are possible. As already mentioned in Section 3, long string segments lead to a clear geometrical signature in CMB temperature anisotropy maps: a line in space across which the temperature jumps by (11).

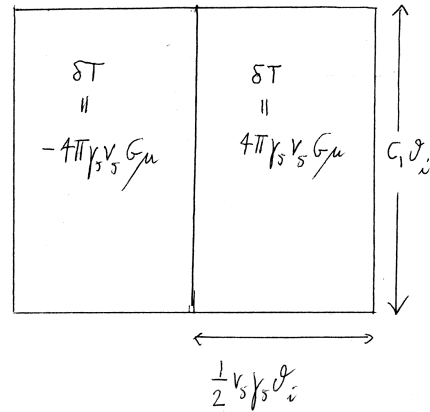


FIG. 4: The temperature pattern on the sky induced by a single string segment.

In fact, due to the finite depth of the conical geometry about the string, a string segment whose world sheet is crossed by our past light cone at time t_i leads to a rectangular pattern in the sky with $\delta T \neq 0$. In the direction on the sky corresponding to the string motion, there is a rectangle of depth

$$\frac{1}{2} \theta_i v_s \gamma_s \quad (15)$$

in front of the string with a positive temperature fluctuations δT (given by (11), whereas behind the string there is a rectangle of similar size the a negative temperature fluctuation of equal magnitude. The width of these rectangles in direction tangent to the string is given by

$$c_1 \theta_i, \quad (16)$$

where θ_i is the angle corresponding to the comoving Hubble radius at the time t_i , and is given by

$$\theta_i = 90^\circ [z(t_i) + 1]^{-1/2}. \quad (17)$$

A sketch of the pattern of an individual string segment is given in Figure 4.

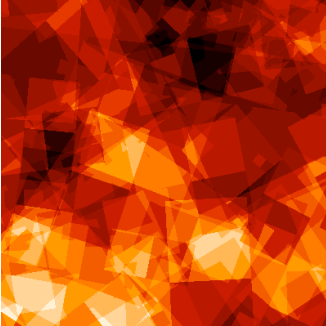


FIG. 5: CMB anisotropy map for a $10^\circ \times 10^\circ$ patch of the sky at $1.5'$ resolution (the specifications are chosen with applications to the SPT and ACT telescope data in mind) in a model in which the fluctuations are given by a scaling distribution of cosmic strings. The color coding indicates the amplitude of the temperature anisotropy.

A scaling network of string segments produces a CMB temperature anisotropy map which can be constructed as follows [48]: given a patch of the sky which is being modelled, we compute the number of string segments present at each Hubble expansion time t_i which are intersected by the portion of the past light cone which the patch of the sky corresponds to. We then choose random centers, directions and velocity vectors for each segment and construct the resulting temperature rectangle in the sky given by the above-mentioned dimensions. The CMB map is a superposition of the rectangles given by the individual string segment. Figure 5 (taken from [48]) presents an image corresponding to a $10^\circ \times 10^\circ$ patch of the sky. Note the large number of small rectangles (early t_i) compared to the larger ones (late t_i).

The best current limits on the cosmic string tension come from comparison of the angular power spectrum of CMB temperature anisotropies [27]. By making use of topological statistics such as Minkowski functionals or edge detection algorithms, improved limits should be

obtainable. Initial studies of CMB maps using Minkowski functionals have been done in [49], and an application of the Canny edge detection algorithm [50] to constructed maps including the contributions from string wakes has shown [48, 51] that an improvement of the limit by one order of magnitude might be achievable with current SPT data.

VI. CMB POLARIZATION PATTERNS FROM A COSMIC STRING WAKE

CMB radiation can be polarized. The polarization data of CMB anisotropies carries interesting cosmological information. Polarization can be decomposed into two independent components which are called E-mode and B-mode polarization. The primordial E-mode polarization has already been discovered [52], but only upper bounds are available on the B-mode. In the near future, experiments such as the SPT [53], ACT [54] and Planck will provide us with greatly improved polarization maps. In this context it is interesting that cosmic strings lead to a specific pattern of CMB polarization, in particular B-mode polarization.

Regular adiabatic fluctuations such as those produced during inflation do not produce any direct B-mode polarization. B-mode polarization in such models can be generated from gravitational waves, or from the lensing of E-mode polarization. In contrast, cosmic strings lead to direct B-mode polarization as was first realized in [55]. The position space signal of B-mode polarization from a string was studied in detail in [56].

CMB polarization is induced by the CMB photons from last scattering crossing a cosmic string wake. Only the quadrupole component Q of the CMB induces polarization. The wake is an overdensity of matter, including baryonic matter. Hence, it also represents an overdensity of free electrons. The CMB photons Compton scatter off of the free electrons, and this process induces CMB polarization. Each wake which is intersected by our past light cone leads to a rectangle in the sky with extra CMB polarization. The angular dimensions of this wake-induced rectangle for a wake created at time t_i are

$$[c_1 \times v_s \gamma_s] \theta_i^2 \quad (18)$$

(as long as the time t when the past light cone intersects the wake is significantly smaller than t_0 - for the general formula the reader is referred to in [57]). Across the rectangle in the sky, the polarization direction is roughly constant. The magnitude P is proportional to Q , to the Thompson cross section, to the width of the wake (which in turn depends on $G\mu$ and on the times t_i and t), to the free electron fraction $f(t)$ at the time t , and to the overall baryon energy fraction Ω_B . Inserting numbers, the result is [56]

$$\frac{P}{Q}(t, t_i) \sim f(t) G\mu v_s \gamma_s \Omega_B \left(\frac{z(t) + 1}{10^3} \right)^2 \left(\frac{z(t_i) + 1}{10^3} \right)^{1/2} 10^7. \quad (19)$$

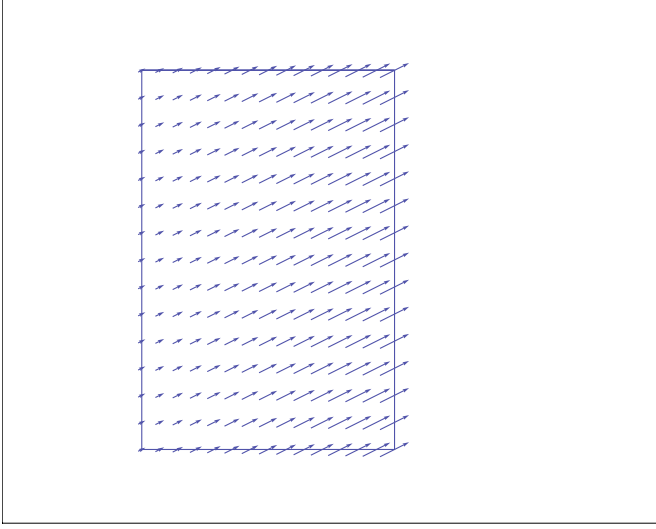


FIG. 6: Sketch of the polarization pattern induced by a cosmic string wake. Shown is a portion of the sky, e.g. $10^\circ \times 10^\circ$, and the polarization which the wake induces. The direction of the arrows indicates the polarization direction, the length of the arrow gives the magnitude.

The above is the mean amplitude across the rectangle. The amplitude increases linearly moving away from the position of the string. The pattern is sketched in Fig. 6 (taken from [56]).

The important point is that, as discussed in detail in [57], the mean amplitude of the induced E and B mode polarizations are the same. Cosmic string wakes thus induce directly B mode polarization, unlike standard adiabatic fluctuations. Hence, the search for B mode polarization is a very important current goal for observational cosmology. The discovery of such polarization could give us a lot of very important information about the early universe. It could confirm the existence of cosmic strings (this is the point emphasized in this article). If any discovered B mode polarization could be shown to be due to gravitational waves, it could shed light on the origin of primordial gravitational waves. A roughly scale invariant spectrum of such waves is predicted not only by inflationary cosmology, but also by a scaling solution of cosmic string loops, and in fact with an amplitude larger than what is predicted in the simplest inflationary models. A discovery of a gravitational wave spectrum with a slight blue tilt would rule out all inflationary models based General Relativity with matter satisfying the usual energy conditions, and it would [58] verify a key prediction of string gas cosmology (see [59] for a more detailed discussion of these points).

The angular power spectrum of string wake-induced B-mode CMB polarization was computed recently in [57]. The spectrum is almost degenerate with that of B-mode polarization induced by lensing. This is another example of the message that in order to detect signals from string wakes, one needs to analyze data in position space.

VII. IMPRINTS OF COSMIC STRINGS IN 21CM SURVEYS

The final window to probe for the possible existence of cosmic strings which we discuss in this article is the window which 21cm redshift surveys provide. These surveys provide, in addition to many other purposes, a means of probing the distribution of baryonic matter during the dark ages, i.e. before the time of star formation. Since 21cm redshift maps are three-dimensional (two dimensions the angles in the sky, the third dimension the redshift), they provide potentially much more information than two dimensional CMB maps.

Before star formation (but after recombination), baryonic matter is almost entirely in the form of neutral hydrogen. Neutral hydrogen has a hyperfine transition line with a wavelength of 21cm. If photons of the cosmic microwave background travel through a cloud of neutral hydrogen, there will be either absorption or emission of 21cm radiation - absorption if the CMB temperature is larger than the gas temperature in the cloud, emission if the gas temperature is larger. Since cosmic string wakes are overdensities of neutral hydrogen, they will lead to a larger 21cm signal.

The 21cm signal of a single string wake was discussed in [60] (see [61] for initial studies of the imprints of cosmic strings in the 21cm background, and see [62] for a general overview of the physics of 21cm surveys). The geometry of the string-induced pattern is very special: extended in the two angular directions and thin in redshift direction. The geometry is sketched in Figure 7 (taken from [60]). On the left side of the figure is a space-time sketch showing the location of the string wake as a function of time, and the past light cone of our observer intersecting the wake. On the right side of the figure is the corresponding signal in redshift space. The horizontal axes on both sides of the figure are the same. The vertical axis is time on the left graph and redshift on the right graph. The signal of the string wake is a thin wedge, roughly but not quite perpendicular to the redshift axis. Within the region of the wedge there is extra 21cm absorption (or emission if $G\mu$ were to be large). The mean thickness of the wedge depends on $G\mu$ since it is determined by the width of the wake. On the other hand, it turns out the the amplitude of the signal is independent of $G\mu$. Thus, if a telescope with excellent redshift resolution were available, the 21cm window would be an excellent one to search for lower tension strings.

The amplitude of the effect of the string wake is given by

$$T_b(\nu) = T_S(1 - e^{-\tau_\nu}) + T_\gamma(\nu)e^{-\tau_\nu}, \quad (20)$$

where T_S is the “spin temperature” of the hydrogen atoms in the gas cloud, and T_γ is the CMB temperature, τ_ν is the dimensionless optical depth, and ν is the frequency. The second term describes the absorption of the primordial CMB photons, the first term yields the emission.

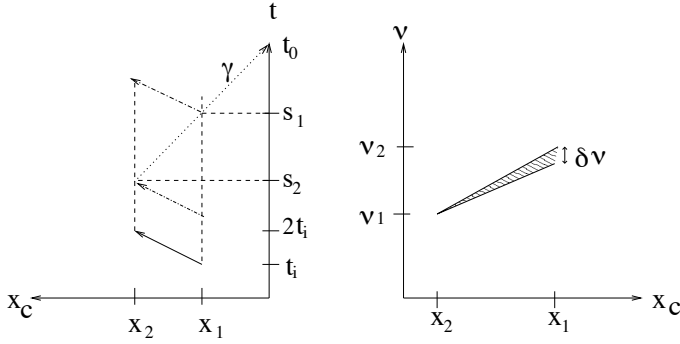


FIG. 7: Geometry of the 21cm signal of a cosmic string wake. The left side shows a space-time sketch with the horizontal axis being comoving spatial coordinate and the vertical axis conformal time) of a wake created at time t_i . The string segment “lives” until the time $2t_i$. Its initial and final positions are x_1 and x_2 , respectively. The wake extends from x_1 to x_2 . Its thickness increases linearly from x_1 to x_2 . The past light cone (indicated by the line labelled γ) intersects the string wake. In the example shown, the past light cone intersects the leading (thin) edge of the wake earlier than the trailing edge. Thus, 21cm photons from the leading edge are redshifted more than those from the trailing edge. This generates a characteristic wedge of extra 21cm absorption / emission due to the string wake in redshift maps. This is sketched on the left of the figure. Here, the horizontal axis is the same comoving spatial coordinate as in the left side, and the vertical axis is the detected 21cm frequency.

The spin temperature determines the excitation level of the hydrogen atoms and is related to the gas temperature T_K in the wake via a collision coefficient x_c (see [62] for the exact equation). We are interested in the difference δT_b between (20) and the CMB temperature, redshifted to the present time:

$$\delta T_b(\nu) = \frac{T_b(\nu) - T_\gamma(\nu)}{1 + z}, \quad (21)$$

which yields

$$\delta T_b(\nu) = T_S \frac{x_c}{1 + x_c} \left(1 - \frac{T_\gamma}{T_K}\right) \tau_\nu (1 + z)^{-1}. \quad (22)$$

The optical depth is proportional to the width of the wake and to the line profile, the broadening of the line due to the varying time of travel of photons emitted at different points in the wake. The line profile is inverse proportional to the width. Hence, the effect of the width (and hence of $G\mu$) cancels out of the amplitude. Inserting numbers, one obtains

$$\delta T_b(\nu) \sim 200 \text{ mK} \text{ for } z + 1 = 30, \quad (23)$$

a very large effect (for details the reader is referred to [60]).

Since string wakes produce such a distinctive geometrical pattern, one should search for strings making use of statistics which are sensitive to this pattern. The use of

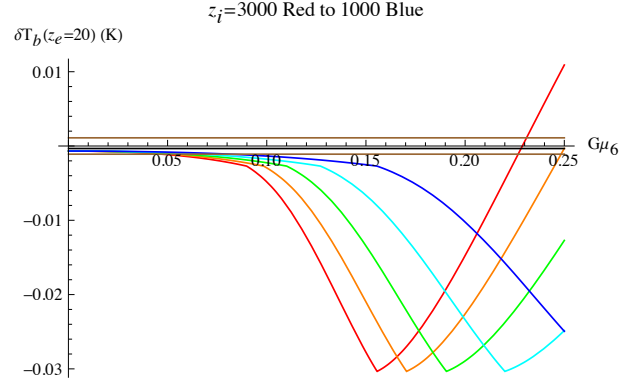


FIG. 8: Pixel amplitude of the string wake signal (vertical axis) as a function of $G\mu$ (horizontal axis) for various values of the wake formation redshift z_i , for the past light cone crossing the wake at redshift 20, just before reionization. For very large values of $G\mu$ the kinetic temperature of the baryons in the wake is larger than the CMB temperature and the string signal is in emission. For smaller values of $G\mu$ the signal is in absorption. The string signal would asymptote to a constant amplitude were it not for the effect of diffusion. This leads to a decrease of the string wake signal for very low values of the tension. As the figure shows, the string signal remains larger than the noise (the almost horizontal lines) to values of $G\mu$ one order of magnitude smaller than the current upper bound.

Minkowski functionals for this purpose has been explored in [63]. One could also apply edge detection algorithms.

The calculations summarized above were done neglecting the thermal velocities of the baryons before they start falling into the wake. At early redshifts and for low values of $G\mu$ this is clearly not justified. Including these initial thermal velocities will lead to the wake being diffuse. This will increase the width of the wake (we speak of a “diffuse string wake”), but will decrease the pixel by pixel amplitude. The effect at a point in the sky integrated over redshift remains the same, as was studied in [64].

What range of values of $G\mu$ might be visible in 21cm surveys? A conservative criterion for visibility is that the pixel signal due to a string wake be larger than the expected pixel noise. The study of [64] indicates that values of $G\mu$ one order of magnitude smaller than the current limit might be visible. This is depicted in Figure 8 (taken from [64]) which shows the string wave signal as a function of $G\mu$ for various values in the redshift z_i when the wake is laid down, and for a fixed redshift $z = 20$ when our past light cone intersects the wake, compared to the noise (the almost horizontal lines to the top and bottom of the horizontal axis). Note that the noise is an increasing function as the pixel size decreases. Low values of $G\mu$ require smaller pixel sizes and hence the noise level will be higher. Making use of algorithms sensitive to the particular geometrical pattern of the string wake signal will allow us to probe significantly smaller values of $G\mu$.

We close this section with a couple of final comments.

First, the amplitude of the 21cm signal from a cosmic string loop is, as was studied in [65] larger by a factor of 16 compared to the amplitude of the wake signal, the reason being that the overdensity is larger by that factor (contraction occurs in three instead of just one dimension). On the other hand, there is no distinctive geometrical signature of the loop signal, and hence it will be more difficult to tease apart the loop signal from point source noise. Second, the two-dimensional angular power spectrum of the string wake signal has also been calculated [66]. However, the result does not show specific stringy features.

VIII. CONCLUSIONS

Since the seeds of the cosmological fluctuations which we observe today have been laid down in the very early universe, these fluctuations may carry imprints of the physics at the earliest times, and this means the physics at highest energy scales. As an example, we have studied how some observational windows can be used to probe for the possible existence of cosmic strings produced by particle physics theories beyond the Standard Model.

One of the important conclusions is that the signals of strings are more prominent in position space than in Fourier space. Hence, to find or constrain strings it is important to use good position space statistics (some attempts were described in the text). For CMB temperature anisotropy maps the distinctive signal of string wakes is line discontinuities, for CMB polarization maps it is rectangles on the sky with a polarization amplitude which increases linearly in one direction, and whose polarization angle is roughly constant. In particular, there is direct B-mode polarization. In the case of 21cm redshift maps, string wakes lead to wedges which are extended across the angular directions but thin along the redshift axis. The amplitude of the position space signals is typically independent of the unknown constant N which describes the string scaling solution, except when overlaps on the sky of the signals of different string wakes are important.

We have assumed here, for simplicity, that the strings

are topologically stable and non-superconducting. Two interesting avenues of extension are to consider superconducting strings [67] for which electromagnetic interactions are important and will lead to a rather different cosmological scenario (see e.g. [68] for a review) and non-topological strings.

Non-topological strings (see [69] for a review) are string solutions which are unstable in the vacuum. However, as first discussed in [70] and more recently in [71] such strings can be stabilized in a plasma. In fact, even the Standard Model of particle physics admits strings (namely the electroweak Z-string and the pion string of the low-energy sigma model of QCD) which can be stabilized by the electromagnetic plasma present before the time of recombination. In this case, they will form in the early universe like topological strings, and they can play a similar cosmological role.

Strings are not the only type of defect solutions. We have focused on string solutions since they are the cosmologically most interesting ones. Models with domain walls are ruled out if the energy scale is beyond the scale of the LHC since a single domain wall would overclose the universe [72]. Gauge monopoles are also ruled out by overclosure considerations for high energy scale walls [73].

Finally, it is important to mention that all our studies of cosmic string signals have been in the context of a one-scale toy model for the distribution of strings. It would be interesting to study the string signals using the inputs of actual string evolution simulations. There are clearly lots of interesting projects to be undertaken.

Acknowledgments

I wish to thank Prof. Pauchy Hwang for the invitation to contribute to one of the first issues of “Universe”. I wish to thank Rebecca Danos for permission to use various figures drawn from [48, 56, 60], and to Oscar Hernandez for permission to use Figure 8 which is taken from [64]. This research has been supported in part by an NSERC Discovery Grant and by funds from the Canada Research Chair program.

-
- [1] Guth AH, “The Inflationary Universe: A Possible Solution To The Horizon And Flatness Problems,” *Phys. Rev. D* **23**, 347 (1981).
 - [2] R. H. Brandenberger and C. Vafa, “Superstrings In The Early Universe,” *Nucl. Phys. B* **316**, 391 (1989).; A. Nayeri, R. H. Brandenberger and C. Vafa, “Producing a scale-invariant spectrum of perturbations in a Hagedorn phase of string cosmology,” *Phys. Rev. Lett.* **97**, 021302 (2006) [arXiv:hep-th/0511140]; R. H. Brandenberger, A. Nayeri, S. P. Patil and C. Vafa, “String gas cosmology and structure formation,” *Int. J. Mod. Phys. A* **22**, 3621 (2007) [hep-th/0608121];
 - R. H. Brandenberger, “String Gas Cosmology,” arXiv:0808.0746 [hep-th].
 - [3] J. Khoury, B. A. Ovrut, P. J. Steinhardt and N. Turok, “The ekpyrotic universe: Colliding branes and the origin of the hot big bang,” *Phys. Rev. D* **64**, 123522 (2001) [arXiv:hep-th/0103239].
 - [4] D. Wands, “Duality invariance of cosmological perturbation spectra,” *Phys. Rev. D* **60**, 023507 (1999) [arXiv:gr-qc/9809062]; F. Finelli and R. Brandenberger, “On the generation of a scale-invariant spectrum of adiabatic fluctuations in cosmological models with a contracting phase,” *Phys. Rev.*

- D **65**, 103522 (2002) [arXiv:hep-th/0112249].
- [5] T. W. B. Kibble, "Topology of Cosmic Domains and Strings," J. Phys. A **9**, 1387 (1976).
- [6] R. H. Brandenberger, "Searching for Cosmic Strings in New Observational Windows," arXiv:1301.2856 [astro-ph.CO].
- [7] V. F. Mukhanov, H. A. Feldman and R. H. Brandenberger, "Theory of cosmological perturbations. Part 1. Classical perturbations. Part 2. Quantum theory of perturbations. Part 3. Extensions," Phys. Rept. **215**, 203 (1992).
- [8] R. H. Brandenberger, "Lectures on the theory of cosmological perturbations," Lect. Notes Phys. **646**, 127 (2004) [arXiv:hep-th/0306071].
- [9] T. W. B. Kibble, "Some Implications of a Cosmological Phase Transition," Phys. Rept. **67**, 183 (1980);
T. W. B. Kibble, "Phase Transitions In The Early Universe," Acta Phys. Polon. B **13**, 723 (1982).
- [10] A. Albrecht and N. Turok, "Evolution Of Cosmic Strings," Phys. Rev. Lett. **54**, 1868 (1985);
D. P. Bennett and F. R. Bouchet, "Evidence For A Scaling Solution In Cosmic String Evolution," Phys. Rev. Lett. **60**, 257 (1988);
B. Allen and E. P. S. Shellard, "Cosmic String Evolution: A Numerical Simulation," Phys. Rev. Lett. **64**, 119 (1990);
C. Ringeval, M. Sakellariadou and F. Bouchet, "Cosmological evolution of cosmic string loops," JCAP **0702**, 023 (2007) [arXiv:astro-ph/0511646];
V. Vanchurin, K. D. Olum and A. Vilenkin, "Scaling of cosmic string loops," Phys. Rev. D **74**, 063527 (2006) [arXiv:gr-qc/0511159];
J. J. Blanco-Pillado, K. D. Olum and B. Shlaer, "Large parallel cosmic string simulations: New results on loop production," Phys. Rev. D **83**, 083514 (2011) [arXiv:1101.5173 [astro-ph.CO]].
- [11] A. Vilenkin, "Cosmic Strings And Domain Walls," Phys. Rept. **121**, 263 (1985);
A. Vilenkin and E.P.S. Shellard, *Cosmic Strings and other Topological Defects* (Cambridge Univ. Press, Cambridge, 1994).
- [12] M. B. Hindmarsh and T. W. B. Kibble, "Cosmic strings," Rept. Prog. Phys. **58**, 477 (1995) [arXiv:hep-ph/9411342].
- [13] R. H. Brandenberger, "Topological defects and structure formation," Int. J. Mod. Phys. A **9**, 2117 (1994) [arXiv:astro-ph/9310041].
- [14] N. Turok and R. H. Brandenberger, "Cosmic Strings And The Formation Of Galaxies And Clusters Of Galaxies," Phys. Rev. D **33**, 2175 (1986);
H. Sato, "Galaxy Formation by Cosmic Strings," Prog. Theor. Phys. **75**, 1342 (1986);
A. Stebbins, "Cosmic Strings and Cold Matter", Ap. J. (Lett.) **303**, L21 (1986).
- [15] T. Vachaspati and A. Vilenkin, "Gravitational Radiation from Cosmic Strings," Phys. Rev. D **31**, 3052 (1985).
- [16] E. Witten, "Cosmic Superstrings," Phys. Lett. B **153**, 243 (1985).
- [17] E. J. Copeland, R. C. Myers and J. Polchinski, "Cosmic F- and D-strings," JHEP **0406**, 013 (2004) [arXiv:hep-th/0312067].
- [18] Y. B. Zeldovich, "Cosmological fluctuations produced near a singularity," Mon. Not. Roy. Astron. Soc. **192**, 663 (1980).
- [19] A. Vilenkin, "Cosmological Density Fluctuations Produced By Vacuum Strings," Phys. Rev. Lett. **46**, 1169 (1981) [Erratum-ibid. **46**, 1496 (1981)].
- [20] R. H. Brandenberger and N. Turok, "Fluctuations From Cosmic Strings And The Microwave Background," Phys. Rev. D **33**, 2182 (1986).
- [21] J. Magueijo, A. Albrecht, D. Coulson and P. Ferreira, "Doppler peaks from active perturbations," Phys. Rev. Lett. **76**, 2617 (1996) [arXiv:astro-ph/9511042];
U. L. Pen, U. Seljak and N. Turok, "Power spectra in global defect theories of cosmic structure formation," Phys. Rev. Lett. **79**, 1611 (1997) [arXiv:astro-ph/9704165];
L. Perivolaropoulos, "Spectral Analysis Of Microwave Background Perturbations Induced By Cosmic Strings," Astrophys. J. **451**, 429 (1995) [arXiv:astro-ph/9402024].
- [22] P. D. Mauskopf *et al.* [Boomerang Collaboration], "Measurement of a Peak in the Cosmic Microwave Background Power Spectrum from the North American test flight of BOOMERANG," Astrophys. J. **536**, L59 (2000) [arXiv:astro-ph/9911444].
- [23] C. L. Bennett *et al.*, "First Year Wilkinson Microwave Anisotropy Probe (WMAP) Observations: Preliminary Maps and Basic Results," Astrophys. J. Suppl. **148**, 1 (2003) [arXiv:astro-ph/0302207].
- [24] J. E. Ruhl *et al.* [The SPT Collaboration], "The South Pole Telescope," Proc. SPIE Int. Soc. Opt. Eng. **5498**, 11 (2004) [arXiv:astro-ph/0411122].
- [25] A. Kosowsky [the ACT Collaboration], "The Atacama Cosmology Telescope Project: A Progress Report," New Astron. Rev. **50**, 969 (2006) [arXiv:astro-ph/0608549].
- [26] P. A. R. Ade *et al.* [Planck Collaboration], "Planck 2013 results. I. Overview of products and scientific results," arXiv:1303.5062 [astro-ph.CO].
- [27] J. Urrestilla, N. Bevis, M. Hindmarsh and M. Kunz, "Cosmic string parameter constraints and model analysis using small scale Cosmic Microwave Background data," JCAP **1112**, 021 (2011) [arXiv:1108.2730 [astro-ph.CO]];
C. Dvorkin, M. Wyman and W. Hu, "Cosmic String constraints from WMAP and the South Pole Telescope," Phys. Rev. D **84**, 123519 (2011) [arXiv:1109.4947 [astro-ph.CO]];
P. A. R. Ade *et al.* [Planck Collaboration], "Planck 2013 results. XXV. Searches for cosmic strings and other topological defects," arXiv:1303.5085 [astro-ph.CO].
- [28] L. Pogosian, S. H. H. Tye, I. Wasserman and M. Wyman, "Observational constraints on cosmic string production during brane inflation," Phys. Rev. D **68**, 023506 (2003) [Erratum-ibid. D **73**, 089904 (2006)] [arXiv:hep-th/0304188];
M. Wyman, L. Pogosian and I. Wasserman, "Bounds on cosmic strings from WMAP and SDSS," Phys. Rev. D **72**, 023513 (2005) [Erratum-ibid. D **73**, 089905 (2006)] [arXiv:astro-ph/0503364];
A. A. Fraisse, "Limits on Defects Formation and Hybrid Inflationary Models with Three-Year WMAP Observations," JCAP **0703**, 008 (2007) [arXiv:astro-ph/0603589];
U. Seljak, A. Slosar and P. McDonald, "Cosmological parameters from combining the Lyman-alpha forest with CMB, galaxy clustering and SN constraints," JCAP **0610**, 014 (2006) [arXiv:astro-ph/0604335];
R. A. Battye, B. Garbrecht and A. Moss, "Constraints on supersymmetric models of hybrid inflation," JCAP

- 0609**, 007 (2006) [arXiv:astro-ph/0607339];
 R. A. Battye, B. Garbrecht, A. Moss and H. Stoica, “Constraints on Brane Inflation and Cosmic Strings,” *JCAP* **0801**, 020 (2008) [arXiv:0710.1541 [astro-ph]];
 N. Bevis, M. Hindmarsh, M. Kunz and J. Urrestilla, “CMB power spectrum contribution from cosmic strings using field-evolution simulations of the Abelian Higgs model,” *Phys. Rev. D* **75**, 065015 (2007) [arXiv:astro-ph/0605018];
 N. Bevis, M. Hindmarsh, M. Kunz and J. Urrestilla, “Fitting CMB data with cosmic strings and inflation,” *Phys. Rev. Lett.* **100**, 021301 (2008) [astro-ph/0702223 [ASTRO-PH]];
 R. Battye and A. Moss, “Updated constraints on the cosmic string tension,” *Phys. Rev. D* **82**, 023521 (2010) [arXiv:1005.0479 [astro-ph.CO]].
- [29] V. F. Mukhanov and G. V. Chibisov, “Quantum Fluctuation and Nonsingular Universe. (In Russian),” *JETP Lett.* **33**, 532 (1981) [*Pisma Zh. Eksp. Teor. Fiz.* **33**, 549 (1981)].
- [30] R. H. Brandenberger, “Unconventional Cosmology,” arXiv:1203.6698 [astro-ph.CO];
 R. H. Brandenberger, “Introduction to Early Universe Cosmology,” *PoS ICFI* **2010**, 001 (2010) [arXiv:1103.2271 [astro-ph.CO]].
- [31] R. Jeannerot, “A Supersymmetric SO(10) Model with Inflation and Cosmic Strings,” *Phys. Rev. D* **53**, 5426 (1996) [arXiv:hep-ph/9509365];
 R. Jeannerot, J. Rocher and M. Sakellariadou, “How generic is cosmic string formation in SUSY GUTs,” *Phys. Rev. D* **68**, 103514 (2003) [arXiv:hep-ph/0308134].
- [32] S. Sarangi and S. H. H. Tye, “Cosmic string production towards the end of brane inflation,” *Phys. Lett. B* **536**, 185 (2002) [arXiv:hep-th/0204074].
- [33] V. S. Berezinsky, V. I. Dokuchaev and Y. N. Eroshenko, “Dense DM clumps seeded by cosmic string loops and DM annihilation,” *JCAP* **1112**, 007 (2011) [arXiv:1107.2751 [astro-ph.HE]];
 M. Anthonisen, R. Brandenberger and P. Scott, in preparation.
- [34] B. Shlaer, A. Vilenkin and A. Loeb, “Early structure formation from cosmic string loops,” *JCAP* **1205**, 026 (2012) [arXiv:1202.1346 [astro-ph.CO]].
- [35] A. Vilenkin, “Gravitational Field Of Vacuum Domain Walls And Strings,” *Phys. Rev. D* **23**, 852 (1981);
 R. Gregory, “Gravitational Stability of Local Strings,” *Phys. Rev. Lett.* **59**, 740 (1987).
- [36] N. Kaiser and A. Stebbins, “Microwave Anisotropy Due To Cosmic Strings,” *Nature* **310**, 391 (1984).
- [37] J. R. Gott, III, “Gravitational lensing effects of vacuum strings: Exact solutions,” *Astrophys. J.* **288**, 422 (1985).
- [38] J. C. R. Magueijo, “Inborn metric of cosmic strings,” *Phys. Rev. D* **46**, 1368 (1992).
- [39] J. Silk and A. Vilenkin, “Cosmic Strings And Galaxy Formation,” *Phys. Rev. Lett.* **53**, 1700 (1984).
- [40] Y. B. Zeldovich, “Gravitational instability: An Approximate theory for large density perturbations,” *Astron. Astrophys.* **5**, 84 (1970).
- [41] R. H. Brandenberger, L. Perivolaropoulos and A. Stebbins, “Cosmic Strings, Hot Dark Matter And The Large Scale Structure Of The Universe,” *Int. J. Mod. Phys. A* **5**, 1633 (1990);
 L. Perivolaropoulos, R. H. Brandenberger and A. Stebbins, “Dissipationless Clustering Of Neutrinos In Cosmic String Induced Wakes,” *Phys. Rev. D* **41**, 1764 (1990).
- [42] L. Perivolaropoulos, “COBE versus cosmic strings: An Analytical model,” *Phys. Lett. B* **298**, 305 (1993) [arXiv:hep-ph/9208247];
 L. Perivolaropoulos, “Statistics of microwave fluctuations induced by topological defects,” *Phys. Rev. D* **48**, 1530 (1993) [arXiv:hep-ph/9212228].
- [43] M. Rees, “Baryon concentrations in string wakes at $z \geq 200$: implications for galaxy formation and large-scale structure,” *Mon. Not. R. astr. Soc.* **222**, 27p (1986);
 T. Vachaspati, “Cosmic Strings and the Large-Scale Structure of the Universe,” *Phys. Rev. Lett.* **57**, 1655 (1986);
 A. Stebbins, S. Veeraraghavan, R. H. Brandenberger, J. Silk and N. Turok, “Cosmic String Wakes,” *Astrophys. J.* **322**, 1 (1987);
 J. C. Charlton, “Cosmic String Wakes and Large Scale Structure,” *Astrophys. J.* **325**, 52 (1988);
 T. Hara and S. Miyoshi, “Formation of the First Systems in the Wakes of Moving Cosmic Strings,” *Prog. Theor. Phys.* **77**, 1152 (1987);
 T. Hara and S. Miyoshi, “Flareup of the Universe After Z Approximately 10^{**2} for Cosmic String Model,” *Prog. Theor. Phys.* **78**, 1081 (1987);
 T. Hara and S. Miyoshi, “Large Scale Structures and Streaming Velocities Due to Open Cosmic Strings,” *Prog. Theor. Phys.* **81**, 1187 (1989).
- [44] K. R. Mecke, T. Buchert, H. Wagner, “Robust morphological measures for large scale structure in the universe,” *Astron. Astrophys.* **288**, 697-704 (1994). [astro-ph/9312028];
 J. Schmalzing and T. Buchert, “Beyond genus statistics: a unifying approach to the morphology of cosmic structure,” *Astrophys. J.* **482**, L1 (1997) [arXiv:astro-ph/9702130];
 J. Schmalzing, T. Buchert, A. L. Melott, V. Sahni, B. S. Sathyaprakash and S. F. Shandarin, “Disentangling the cosmic web I: morphology of isodensity contours,” *Astrophys. J.* **526**, 568 (1999) [arXiv:astro-ph/9904384].
- [45] H. Trac, D. Mitsouras, P. Hickson and R. H. Brandenberger, “Topology of the Las Campanas redshift survey,” *Mon. Not. Roy. Astron. Soc.* **330**, 531 (2002) [astro-ph/0007125];
 D. Mitsouras, R. H. Brandenberger and P. Hickson, “Topological statistics and the LMT galaxy redshift project,” [astro-ph/9806360].
- [46] F. Duplessis and R. Brandenberger, “Note on Structure Formation from Cosmic String Wakes,” *JCAP* **1304**, 045 (2013) [arXiv:1302.3467 [astro-ph.CO]].
- [47] Y. Omori, R. Brandenberger and T. Webb, in preparation (2014).
- [48] R. J. Danos and R. H. Brandenberger, “Canny Algorithm, Cosmic Strings and the Cosmic Microwave Background,” *Int. J. Mod. Phys. D* **19**, 183 (2010) [arXiv:0811.2004 [astro-ph]].
- [49] D. Novikov, H. A. Feldman and S. F. Shandarin, “Minkowski functionals and cluster analysis for CMB maps,” *Int. J. Mod. Phys. D* **8**, 291 (1999) [arXiv:astro-ph/9809238];
 C. Hikage, E. Komatsu and T. Matsubara, “Primordial Non-Gaussianity and Analytical Formula for Minkowski Functionals of the Cosmic Microwave Background and Large-scale Structure,” *Astrophys. J.* **653**, 11 (2006) [arXiv:astro-ph/0607284];

- S. Winitzki and A. Kosowsky, “Minkowski functional description of microwave background Gaussianity,” *New Astron.* **3**, 75 (1998) [arXiv:astro-ph/9710164].
- [50] J. Canny, “A computational approach to edge detection,” *IEEE Trans. Pattern Analysis and Machine Intelligence* **8**, 679 (1986).
- [51] S. Amsel, J. Berger and R. H. Brandenberger, “Detecting Cosmic Strings in the CMB with the Canny Algorithm,” *JCAP* **0804**, 015 (2008) [arXiv:0709.0982 [astro-ph]]; A. Stewart and R. Brandenberger, “Edge Detection, Cosmic Strings and the South Pole Telescope,” *JCAP* **0902**, 009 (2009) [arXiv:0809.0865 [astro-ph]].
- [52] J. Kovac, E. M. Leitch, CPryke, J. E. Carlstrom, N. W. Halverson and W. L. Holzapfel, “Detection of polarization in the cosmic microwave background using DASI,” *Nature* **420**, 772 (2002) [astro-ph/0209478].
- [53] J. E. Austermann, K. A. Aird, J. A. Beall, D. Becker, A. Bender, B. A. Benson, L. E. Bleem and J. Britton *et al.*, “SPTpol: an instrument for CMB polarization measurements with the South Pole Telescope,” *Proc. SPIE Int. Soc. Opt. Eng.* **8452**, 84520E (2012) [arXiv:1210.4970 [astro-ph.IM]].
- [54] M. D. Niemack, P. A. R. Ade, J. Aguirre, F. Barrientos, J. A. Beall, J. R. Bond, J. Britton and H. M. Cho *et al.*, “ACTPol: A polarization-sensitive receiver for the Atacama Cosmology Telescope,” *Proc. SPIE Int. Soc. Opt. Eng.* **7741**, 77411S (2010) [arXiv:1006.5049 [astro-ph.IM]].
- [55] U. Seljak, U. L. Pen and N. Turok, “Polarization of the Microwave Background in Defect Models,” *Phys. Rev. Lett.* **79**, 1615 (1997) [arXiv:astro-ph/9704231]; U. Seljak and A. Slosar, “B polarization of cosmic microwave background as a tracer of strings,” *Phys. Rev. D* **74**, 063523 (2006) [arXiv:astro-ph/0604143]; L. Pogosian, I. Wasserman and M. Wyman, “On vector mode contribution to CMB temperature and polarization from local strings,” arXiv:astro-ph/0604141; L. Pogosian and M. Wyman, “B-modes from Cosmic Strings,” *Phys. Rev. D* **77**, 083509 (2008) [arXiv:0711.0747 [astro-ph]]; K. Benabed and F. Bernardeau, “Cosmic string lens effects on CMB polarization patterns,” *Phys. Rev. D* **61**, 123510 (2000); J. Garcia-Bellido, R. Durrer, E. Fenu, D. G. Figueroa and M. Kunz, “The local B-polarization of the CMB: a very sensitive probe of cosmic defects,” *Phys. Lett. B* **695**, 26 (2011) [arXiv:1003.0299 [astro-ph.CO]].
- [56] R. J. Danos, R. H. Brandenberger and G. Holder, “A Signature of Cosmic Strings Wakes in the CMB Polarization,” *Phys. Rev. D* **82**, 023513 (2010) [arXiv:1003.0905 [astro-ph.CO]].
- [57] R. Brandenberger, N. Park and G. Salton, “Angular Power Spectrum of B-mode Polarization from Cosmic String Wakes,” arXiv:1308.5693 [astro-ph.CO].
- [58] R. H. Brandenberger, A. Nayeri, S. P. Patil and C. Vafa, “Tensor Modes from a Primordial Hagedorn Phase of String Cosmology,” *Phys. Rev. Lett.* **98**, 231302 (2007) [hep-th/0604126].
- [59] R. H. Brandenberger, “Is the Spectrum of Gravitational Waves the ‘Holy Grail’ of Inflation?,” arXiv:1104.3581 [astro-ph.CO].
- [60] R. H. Brandenberger, R. J. Danos, O. F. Hernandez and G. P. Holder, “The 21 cm Signature of Cosmic String Wakes,” *JCAP* **1012**, 028 (2010) [arXiv:1006.2514 [astro-ph.CO]].
- [61] R. Khatri and B. D. Wandelt, “Cosmic (super)string constraints from 21 cm radiation,” *Phys. Rev. Lett.* **100**, 091302 (2008) [arXiv:0801.4406 [astro-ph]]; A. Berndsen, L. Pogosian and M. Wyman, “Correlations between 21 cm Radiation and the CMB from Active Sources,” arXiv:1003.2214 [astro-ph.CO].
- [62] S. Furlanetto, S. P. Oh and F. Briggs, “Cosmology at Low Frequencies: The 21 cm Transition and the High-Redshift Universe,” *Phys. Rept.* **433**, 181 (2006) [arXiv:astro-ph/0608032].
- [63] E. McDonough and R. H. Brandenberger, “Searching for Signatures of Cosmic String Wakes in 21cm Redshift Surveys using Minkowski Functionals,” *JCAP* **1302**, 045 (2013) [arXiv:1109.2627 [astro-ph.CO]].
- [64] O. F. Hernandez and R. H. Brandenberger, “The 21 cm Signature of Shock Heated and Diffuse Cosmic String Wakes,” *JCAP* **1207**, 032 (2012) [arXiv:1203.2307 [astro-ph.CO]].
- [65] M. Pagano and R. Brandenberger, “The 21cm Signature of a Cosmic String Loop,” *JCAP* **1205**, 014 (2012) [arXiv:1201.5695 [astro-ph.CO]].
- [66] O. F. Hernandez, Y. Wang, R. Brandenberger and J. Fong, “Angular 21 cm Power Spectrum of a Scaling Distribution of Cosmic String Wakes,” *JCAP* **1108**, 014 (2011) [arXiv:1104.3337 [astro-ph.CO]].
- [67] E. Witten, “Superconducting Strings,” *Nucl. Phys. B* **249**, 557 (1985).
- [68] J. P. Ostriker, A. C. Thompson and E. Witten, “Cosmological Effects of Superconducting Strings,” *Phys. Lett. B* **180**, 231 (1986).
- [69] A. Achucarro and T. Vachaspati, “Semilocal and electroweak strings,” *Phys. Rept.* **327**, 347 (2000) [hep-ph/9904229].
- [70] M. Nagasawa and R. H. Brandenberger, “Stabilization of embedded defects by plasma effects,” *Phys. Lett. B* **467**, 205 (1999) [hep-ph/9904261].
- [71] J. Karouby and R. Brandenberger, “Effects of a Thermal Bath of Photons on Embedded String Stability,” *Phys. Rev. D* **85**, 107702 (2012) [arXiv:1203.0073 [hep-th]].
- [72] Y. B. Zeldovich, I. Y. Kobzarev and L. B. Okun, “Cosmological Consequences of the Spontaneous Breakdown of Discrete Symmetry,” *Zh. Eksp. Teor. Fiz.* **67**, 3 (1974) [*Sov. Phys. JETP* **40**, 1 (1974)].
- [73] J. Preskill, “Cosmological Production of Superheavy Magnetic Monopoles,” *Phys. Rev. Lett.* **43**, 1365 (1979).